

## Answers to the reviewers #2

### General comments:

The authors applied some newly developed tracking algorithms for Linear Kinematics Features (LKF) presented in a recent study by the same authors to two model simulations and RGPS data. This approach allows for direct comparison of various metrics of LKF, namely the density, orientation, length, curvature, intersection angles, persistence and growth rates. This study represents a sophisticated assessment of a model's dynamical features. The presentation is clear, the model realism (in terms of those features) convincing, and some interesting results with obvious physical and operational applications. This paper also offers a contribution to a question that has been debated repeatedly in the community as to the ability for the VP rheologies (and derivatives) to capture the power law distributions seen in the satellite observations. I find that the work is sufficient to justify publication in this journal provided that some of the major issues listed below are addressed.

We thank the anonymous referee #2 for the thorough review.

1) **Model tuning.** How much of the results are the results of parameter tuning? The authors should make it much clearer if these two model configurations are their standard model simulations and if there was a tuning procedure to obtain such realistic fits to the observations. Additionally, has this tuning been to the detriment of other characteristics of the model (i.e. thermodynamic characteristics, sea ice concentration, thickness and velocity). A supplementary plot showing how both models perform with regard to these essential sea ice metrics would be welcome. For example it would not be satisfactory to achieve better fit to the dynamics features discussed in the paper to the detriment of this more standard and important features of the sea ice cover.

The model simulations are very expensive, with respect to the resources available to us, so that we did not tune the simulations, but rather used sea ice and ocean model parameters from a coarse simulation with realistic ice distributions (Nguyen et al., 2011, and ITD specific parameters from Ungermann & Losch, 2018). Objective and automated tuning methods require large repetitions of model simulations for different parameter choices and/or ensemble members (Menemenlis et al., 2005; Nguyen et al., 2011; Massonnet et al., 2014; Ungermann et al., 2017; Sumata et al., 2019), which is currently not feasible for resolutions as high as 2km.

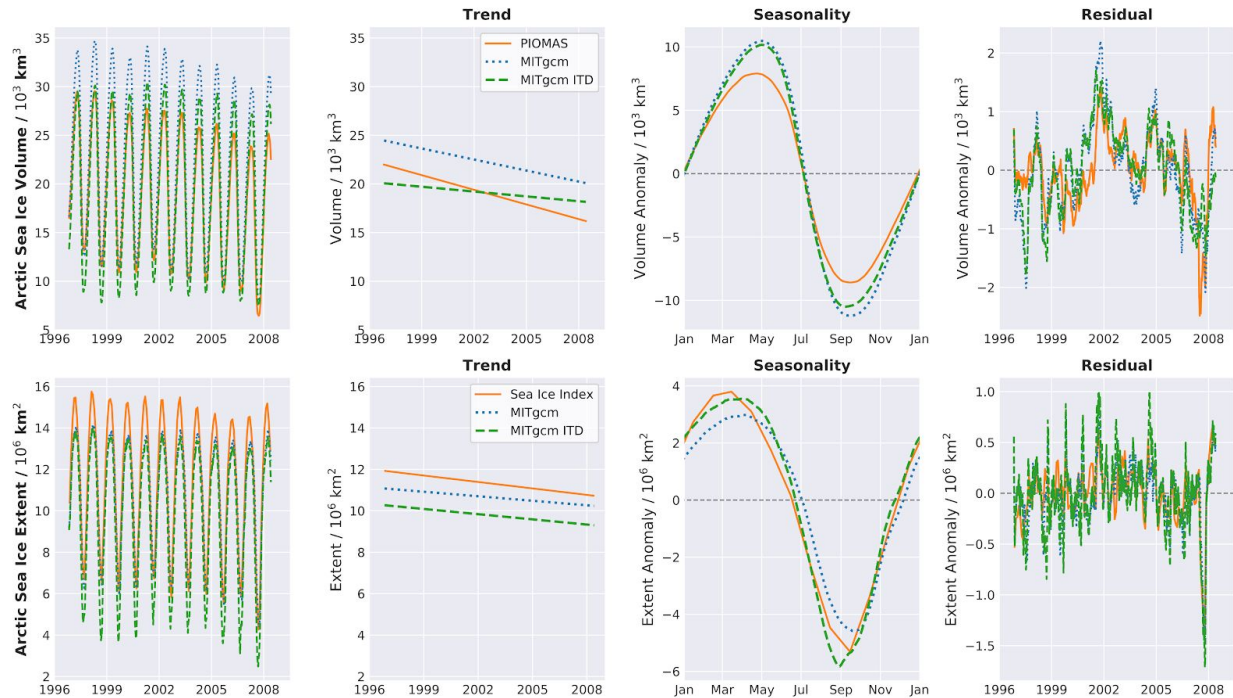


**Figure 1: (top row)** Comparison of Arctic sea ice volume in both model simulations used in our study to the PIOMAS model given as a time series over the entire RGPS period (1996 to 2008) and separated into a linear trend, seasonality and residual. **(lower row)** Same as upper row but for the Arctic sea ice extent from NSIDC. For a full description of the plots see Ungermann & Losch (2018).

As a consequence, both simulations do not reproduce the sea ice volume and extent observed from satellites and reanalysis products in all the details, but agree in the overall trend of sea ice retreat (Fig. 1 of this answer). The lower trend of sea ice volume in the ITD simulations was already reported for the coarse resolution model configuration (Ungermann & Losch, 2018), from which we obtained the ITD specific parameters. The seasonal cycle of sea ice volume is strongly overestimated, which we attributed partly to the 0-layer thermodynamics used in the simulation and to the effect of resolved leads in the simulation. In wintertime, open-ocean is exposed in leads which allows further ice growth even for an ice covered Arctic Ocean. In summertime, ice-ocean interaction along the boundaries of smaller floes accelerate the melting of the ice cover (Horvat et al., 2016). Both model simulations underestimate the maximum sea ice extent, which we attribute to the atmospheric forcing, as both simulations show agree in this underestimation. In conclusion, there is potential to improve the performance of both simulation by tuning model parameters. Due to limited computing resources this task needs to be done in a dedicated study. Our analysis, however, focusses on the RGPS winter coverage, where most data is available from November to April. For this period of the year, both simulations show reasonable sea-ice volume and extent, such that we evaluate the presented drawbacks as non-essential to our analysis.

We added further details to the model description in the manuscript to highlight the fact that both configurations are untuned:

Both model configurations are not tuned to reproduce observed ice distributions due to limited computational resources. Instead, we carried over ocean and sea ice parameters from optimized coarse resolution configurations (Nguyen et al., 2011; Ungermann & Losch, 2018, for ITD specific parameters).

The resulting simulations overestimate the seasonal amplitude of sea ice volume and extent, but their trends are reasonable (not shown). The resulting ocean circulation has not been evaluated in detail, but the wind-driven surface circulation is plausible with strong mesoscale activity, the surface temperature and large scale sea ice distribution follow the prescribed surface forcing as expected. The main role of the ocean model is to provide dynamic bottom boundary conditions to the sea ice model.

And in the discussion section:

The agreement of the scaling analysis and the LKFs statistics between the model simulations and RGPS data may appear almost surprising given that the models have not been tuned at all for these diagnostics. We argue that this model performance is not determined by the large scale distribution of sea ice thickness and concentration, but the plastic model physics. For the plastic physics in VP-models to produce highly intermittent and heterogeneous LKF distributions, high resolution (Spren et al. 2016, Hutter et al. 2018) and a sufficiently accurate solver (Koldunov et al. 2019) are necessary. As long as there is a quasi-closed ice cover, which is the case where and when the RGPS data are available, the plastic physics will produce localized deformation --- even in idealized configurations (Hutter 2015, Heorton et al. 2019) --- and the associated statistics.

**2) References to the literature.** While some sections are well documented, I find other sections do not do justice to previous authors who have worked on this theme. Besides the historical studies by Hibler, Coon, Pritchard, Gray, etc the authors also omit more recent work on the anisotropic rheology of Tsamados et al., Tremblay et al, Lemieux, etc...

We agree that some literature was missing in the first draft of the manuscript and added 17 references in the revision. In particular we focussed on the section of the intersection angles highlighted by the reviewer in the major comment 5) and in the minor comments. Please note that studies of Hibler, Coon, Pritchard had been cited in the paper. We now also include reference to anisotropic rheology.

**3) Model resolution and forcing dependence of the results.** The author present two model runs that differ in their ITD representation (without going too much into the detail of their difference) but fail to present a fair assessment of the sensitivity of their results to the model spatial (and temporal) resolution as well as to the forcing applied. Some definitions (overlap, persistence, etc. . .) are bound to be sensitive to the grid resolution and it would be useful to get a sense of this. An additional, difficult, question that is eluded is the degree of localisation of the LKF in this model. Indeed one crucial quantity of interest of these LKF is their width but the authors fail to discuss that point entirely.

The representation of LKFs is model resolution dependent: with lower resolution there are fewer LKFs and deformation rates are less localized, such that the scaling properties deteriorate (e.g. Spren et al., 2017). The feature-based evaluation presented in this study can only be applied to simulations that explicitly resolve LKFs, which in our experience is only possible for resolutions higher than 5km. This leaves only a small range of model resolution (2 to 5km) for a sensitivity study. Forcing resolution has a similar effect, with higher resolution leads to more localized deformation (Hutter, 2015). With our high resolution configuration it would be possible to test the effect of different atmospheric forcing. Nevertheless, we find that further sensitivity studies are beyond the scope of the manuscript, as the main purpose is to demonstrate a new way to evaluate lead-resolving sea ice simulations. We agree that this

topic is interesting and extensive enough for a dedicated study. We added a paragraph to the Discussions to discuss this effect:

Both model simulations use the same grid and the same atmospheric forcing, which precludes direct inferences of resolution impact on the presented statistics. Here, we comment on expected impact based on previous studies. With increasing horizontal grid spacing, deformation features are more localized and more frequent (Spreen et al., 2016). Thus the number of LKFs, presented in Section 4.1.1, are likely to increase with model resolution along with a decrease in LKF length and growth rates as discussed in the previous paragraph. In idealized experiments, it has been shown that higher spatial resolution of the atmospheric forcing also has the potential to increase the localization of sea-ice deformation (Hutter, 2015). This suggests that also the number of LKFs increase. We speculate, however, that in our simulations this effect is saturated because we already use atmospheric forcing with fairly high resolution (JRA-55,  $0.5625^\circ$ ) that resolves most scales associated with the wind.. To our knowledge, there is no study on the impact of temporal resolution on sea ice deformation. We hypothesize that an increased temporal resolution of the forcing will increase the short-term variability in the evolution LKFs, with direct impact on the LKF growth rates and presence of short-lived LKFs. However, please note that the order of this short-term variability is given by the temporal resolution (hours), which is much smaller than the shortest LKF lifetimes regarded in our study (0-3 days).

We do consider in our study that some parameters of the detection algorithm are resolution dependent. Thus these parameters are scaled accordingly to the model resolution as suggested in Hutter et al., 2019. We now made clear that this adjustment is due to the difference in resolution between the simulations and RGPS data:

The parameters used in the detection algorithm are the same as in Hutter et al. (2019, their Tab. 1), where all parameters marked with <sup>b</sup> are scaled to the reduced model resolution by multiplying with a factor of  $12.5 \text{ km}/6.75 \text{ km} = 1.85$  to account for the resolution difference between the simulations and the RGPS data set.

We agree that the persistence of LKFs is sensitive to the temporal resolution of the atmospheric forcing (in our case 3h) and the time step used by the model (in our case 120s) if lifetimes close to these time scales are regarded. Both time scales are much smaller than the upper bound of the lowest bin of LKF lifetime presented (0 to 3 days). Thus, we do not expect any direct effect on the presented distributions of LKFs lifetimes. We speculate that LKF persistence as well as LKF length and LKF density are sensitive to the number of LKFs and thereby indirectly to the model grid spacing. However, we find that dedicated sensitivity studies are beyond the scope of this study.

We do not discuss the width of LKFs, because LKFs presented in this evaluation are derived from deformation data, which do not allow accurate estimates for the width. Due to the Lagrangian nature of the RGPS data-set deformation features that are one pixel wide can have any width up to 12.5km and multiple pixel wide features are most likely a set of leads. We refrain, therefore, from computing LKF width from the detected LKFs and recommend to use higher resolution satellite products to do so.

**4) Coupling of dynamics with other parts of the model.** The authors treat the problem and the LKFs as if they are completely separate from other components of their model. They make a brief reference to

the ridging scheme and drag coefficients but fail to discuss further how modification of LKFs features could couple to other parts of the model.

We discuss extensively how the resolved LKFs impact on the ice strength and deformation. Besides this link to the dynamics of the sea ice model, there is a clear link to the thermodynamic component of the sea ice model. Once the sea ice cover is opened in a resolved lead, new ice growth is initiated. In the time series of the sea ice volume (Figure 1 of this answer) this effect leads to the overestimation of winter ice volume. Koldunov et al. (2019) showed that the sea ice volume in wintertime increases with increasing number of resolved feature by varying parameters of the EVP solver. In summertime, ice-ocean interaction along the boundaries of smaller floes accelerate the melting of the ice cover (Horvat et al., 2016), which leads to a lower sea ice volume. The heat and freshwater fluxes associated with ice melt and growth in leads might affect the ocean model locally.

There is no feedback of LKFs to drag in the model. As opposed to e.g. Castellani et al (2018), Tsamados et al (2014), LKF density is not a sub grid scale parameterisation, so that previous parameterization of drag as a function of LKF density cannot be used. One could introduce a drag parameterisation (e.g., Lüpkes & Gryanik, 2015) that uses information about the freeboard and characteristic length scale of floes from the simulated sea ice fields that include resolved leads and floes.

We added the following paragraph to the Discussions:

LKFs also affect the thermodynamic component of the sea ice model. Once the sea ice cover is opened in a resolved lead, new ice growth is initiated. Koldunov et al. (2018) found that the wintertime sea ice volume increases with increasing number of resolved features. In summertime, ice-ocean interaction along the boundaries of smaller floes accelerate the melting of the ice cover (Horvat et al., 2016), which leads to a lower sea ice volume. Locally, the heat flux and the freshwater fluxes associated with ice melt and growth in leads may generate horizontal gradients and submesoscale variability (Horvat et al., 2016; Manucharyan & Thompson, 2017). There is no feedback of LKFs to drag in the model. As opposed to, for example, (Castellani et al., 2018; Tsamados et al., 2014), the LKF density is not a sub grid scale parameterisation, so that previous parameterization of drag as a function of LKF density cannot be used. Resolving LKFs allows for a drag parameterisation (e.g., Lüpkes & Gryanik, 2015) that uses information about the free-board and characteristic length scale of floes from the simulated sea ice fields.

5) Final major issue that this study uncovered is that the VP rheology fails to capture the intersection angles as they are observed in the observations. This is an important negative result but others have studied these angles before and should be referenced (Hibler, Hutchings, Pritchard, Grey, Ukita, Heorton, ...etc).

We agree, and now also make more references to previous work. Details are given to the specific comments about Section 4.2.3 LKF intersection angles.

### Specific comments:

P1L6: power law distribution better. Not all power distribution are multi-fractal in nature.

We agree that not all power-law distributions are multi-fractal, but in Section 3 we show that the modeled and observed sea ice deformation shows multi-fractal properties. This information would be lost by replacing it with “power law distributions”, so that we keep “multi-fractal”.

**P1L9: not an ITD simulation but a sea ice simulation with an ITD parameterization**

Changed accordingly.

**P1L17: addressed**

Changed accordingly.

**P2L4: rephrase**

We removed the sentence.

**P2L22: you mean individually?**

We changed the sentence to:

While scaling characteristics give some insight into the underlying material properties of sea ice, their interpretation with respect to individual deformation features is not straightforward (Bouchat & Tremblay, 2017; Hutter et al., 2018).

**P2L29: one of which**

Changed accordingly.

**P2L34: rephrase**

Changed to:

In addition, we test which conclusions about the properties of LKFs can be drawn from a spatio-temporal scaling analysis of sea ice deformation (following, e.g. Rampal et al., 2016; Hutter et al., 2018).

**P3L2: outline?**

Changed accordingly.

**P3L28: Some have argued that power law is in the forcing? How sensitive are your results to the spatio-temporal length scales of the atmo/ocean forcing?**

To our knowledge, only Hutter (2015) studied the impact of the wind forcing resolution on the scaling characteristics of sea ice deformation in idealized experiments. He found that increasing the horizontal grid spacing steepens the power-law of the spatial scaling, but also for coarse resolution forcing one can observe power-law scaling (see Spreen et al. 2017 for JRA-25 forcing with 1.125° resolution). So the magnitude of power-law exponent presented in our study might change slightly if a different wind forcing is used, however, the overall conclusion that the model reproduces the multi-fractal scaling will remain.

**P4L8: we branch -> meaning?**

Rephrased to:

On October 17th, 1995 the simulation with an ice thickness distribution (Thorndike et al., 1975) with 5 thickness categories separated by boundaries at 0.0m, 0.64m, 1.39m, 2.47m, and 4.57m is started.

**P4L13: justify this choice. Cite Landy et al, 2019**

There is extensive literature that ITDs observed in the field are characterized by negative exponential or lognormal distributions. The study mentioned by the reviewer uses these distributions to simulate SAR altimeter echos. In the revised manuscript, we give reference to a dedicated studies on ITDs and a review chapter. The mode of  $\frac{2}{3}$  of lognormal distribution was chosen by visually comparing observed ITDs. We

note here that these distributions are only the initial condition and will evolve during the spin-up. The text is changed:

Therefore, we use the fact that observed ITDs follow log-normal functions (Wadhams,1992; Haas, 2010) and describe the ITD of each grid-cell by a log-normal distribution with a mode of 2/3 of the mean thickness.

**P4L19: bold not a good idea. I suggest run\_ITD run\_noITD**

We agree and replace bold face by quotation marks: "ITD", "noITD".

**P4L32: what boundary?**

The deformation rates that are calculated with the line integral approximation depend on the boundary of the cell along which the integration takes place. Lindsay and Stern (2003) showed that for strongly deformed cells the computed deformation rates depend on the number of vertices, which define the boundary of the cell. They refer to this uncertainty in deformation rates, introduced to the RGPS data set by only 4 vertices per cell, as boundary definition error. We changed the text to make clear that this uncertainty is present in strongly deformed cells:

For an accurate magnitude of the deformation rates and in particular the temporal scaling, only the most sophisticated option (1) can be used as it takes the advection of ice into account and addresses the effect of distorted vertices on the computation of the deformation rates (Lindsay & Stern, 2003) consistently for model and RGPS.

**P5L9: contradicts power law distribution and localisation**

This sentence refers to the parameters of the detection algorithm. As the detection algorithm works in pixel space, all parameters given in pixel units need to be adjusted to different resolution of the input data. We do not see how this contradicts the power-law scaling as the resolution used is always the lower bound of scaling behaviour.

**P5L15: and Weiss et al, 2018 for space-time power laws**

For clarity we refrain to state explicitly the space-time power-laws as a separate equation but refer to the paper:

Sea-ice deformation is known to depend on spatial and temporal scales following a power-law (Weiss, 2013; Weiss & Dansereau, 2017, for spaced-time coupled form), ...

**P5L29: this is not clear here and some repeat of earlier paper might be needed**

We changed to text to be more specific:

The spatio-temporal scaling analysis performed in this paper is based on Lagrangian drift data as suggested in Section 2.3.2. To transfer the RGPS sampling to the model output, we convert the regular gridded velocity output of the model to Lagrangian drift data by integrating trajectories from daily averaged velocity output of the model. Virtual buoys are initialized on the RGPS grid on November 1st of each year (1996-2007). The virtual buoys are advected with the modeled ice drift until mid-May of the following year and their positions are recorded every day.

**P6L9: than ...( $L < L_0/2$ )**

Changed accordingly.

**P6L19: unclear sentences. What two streams are you referring to in this sentence?**

The RGPS Lagrangian data sets is distributed in so-called streams. Each stream refers to one specific constellation of two overfly paths of RADARSAT that overlap in the observed region with a time difference of roughly 3 days. The formulation in the manuscript, therefore, was misleading and changed to:

Note that in this way the positions of drifters that are on both images are updated twice within a time period much shorter than 3 days. The time difference within one overfly (order of minutes) is small compared to the time difference between two different overflies that cover the same region (order of 3days).

**P6L33: Brief algorithm schematic needed in appendix or clear reference to previous paper, section etc. . .**

We included a reference to the Data User's Handbook of RGPS (Kwok & Cunningham, 2014), where detailed information about streams and deformation rate computation by with line integrals can be found. For a more accurate conversion, we take the following processing steps for each RGPS stream (all points that are covered by two consecutive overflies of the satellite, for details see Kwok and Cunningham, 2014): ....

**P7L4: General comment: it would be good to know what tuning you have undergone to achieve such a good fit with the observations.**

We perform no tuning, please see answer to major comment for details.

**P7L5: decreases**

Changed accordingly.

**P7L16: Can you also check the space-time scaling as discussed in Weiss et al, 2018**

With our method we can check the dependence of the spatial scaling exponent to temporal scales and vice versa. With this it is possible to test for space-time coupling as discussed in Weiss & Dansereau (2017). The space-time coupling discussed in Weiss & Dansereau (2017) and also in the original paper Marsan & Weiss (2010) is based on buoy data, from which a proxy for deformation is derived (Rampal et al., 2008). These observations have a coarse resolution, but cover a long time record. For the high-resolution RGPS data-set, we find that this space-time coupling varies strongly from year to year, with years showing the coupling and years not showing the coupling. Averaging over the entire RGPS period, we do not observe clear space-time coupling (to our knowledge also no other study shows the space-time coupling for RGPS). Therefore, we omitted to discuss this coupling in the manuscript and decided to show the multi-fractal properties as discussed in most recent modelling scaling studies (Rampal et al., 2019).

**P8L11: Not clear if it is not good in this study or in Rampal's. Rephrase**

The quality of the power-law fit in our study is comparable to the one in Rampal et al. (2019). For clarity, we therefore removed the statement and the sentence reads now as follows:

The curvature of the structure function of the temporal and spatial scaling exponent follows a power-law (Fig. 3 a and b) as suggested by Rampal et al. (2019).

**P8L16: how does this link with power law exponents? Explain**

We added a sentence to make this clear:

Due to the reduced ice strength, deformation increases yielding to a stronger localization of deformation in space and time and thereby higher scaling exponents.

P9L2: This is slightly too strong as they were developed also to represent some physical characteristics (i.e. stress redistribution...)

We reformulated the statement to be more general:

In summary, the spatio-temporal scaling analysis shows that both model simulations reproduce the observed multi-fractal heterogeneity and intermittency of sea-ice deformation (Marsan et al., 2004; Rampal et al., 2008; Weiss & Dansereau, 2017; Oikkonen et al., 2017) equally well as more sophisticated models that were specifically designed with these characteristics in mind (Girard et al., 2011).

P10L1: Important consideration is how the results presented below scale with model resolution but also with spatio-temporal scales of the forcing fields.

We agree that a discussion of the effect of both model and forcing resolution on the presented statistics is of interest for the reader. As an additional sensitivity study is out of the scope of this manuscript, we add the paragraph already stated in our answer to major comment #3 to the Discussion Section.

P10L9: does not seem significant and also raises questions as to how LKFs are detected in a changing Arctic

Changed to:

The RGPS LKF data-set shows little variation in the number of deformation features in the entire observing period with no clear trend (from 0.015 to 0.0125 LKFs per RGPS observation).

P10L22: any suggestions as to why? Generally little elements of physical explanations of the results are given.

We attribute the lower numbers of LKFs in the noITD simulation to the lack of inhomogeneities in the ice that facilitate sea ice deformation. For the ITD simulation, the different ice strength parameterisation (Rothrock, 1975) introduces inhomogeneities in the ice strength. We already discuss this link in the Discussions. We speculate that the higher seasonal variability in the ITD simulation is caused by a higher sensitivity to variations in the atmospheric forcing (such as storms) due the introduced inhomogeneities.

P10L33: Not clear to me how this relative density is calculated (what unit?) and how you can compare it to MODIS or CS2 information. For CS2 please also cite recent paper by Horvat et al, 2019.

We subdivide the Arctic Ocean in 50x50km boxes and count how many times we find LKF pixels in this box. This frequency is then normalized with the number of RGPS observations within the box, to compensate for the varying coverage of RGPS. To be more clear, we added more information to the caption of Figure 5:

Figure 5. (a,c,e) The density of LKFs in the RGPS data set and the two model simulations for the winters between 1996 and 2008 computed in 50x50km boxes over the Arctic Ocean. The absolute frequency of LKF pixels in a box is normalized by the total number of pixels with deformation in the data set. Only boxes with more than 500 deformation pixels in space and time are shown.

Therefore, the computed frequencies can be compared to lead frequencies derived from MODIS and CryoSat-2 that basically determine the frequency of open water pixels. However, the LKF densities in our study also include pressure ridges, which needs to take into account once comparing both.

Horvat et al. (2019) studies the floe size distribution from CryoSat-2. The number of floes and the spacing between them is needed to directly infer lead densities from the floe size distribution. Since the latter is not given in Horvat et al. (2019) no direct inferences on the lead density is possible, such that we decided not to include this study in our paper.

P13L17: Another possibility is that some of these features are ocean driven (geostrophic current or Eddies). There is extensive recent literature on this in this region,

In the manuscript we already name the Beaufort Gyre as one ocean driver of sea ice deformation in the Beaufort Sea. We agree that eddies generated within the gyre might also play a role in exerting stress on sea ice on small spatial scales. We included this to the text:

We do not observe the increased probability in LKF formation in either simulations, which may suggest that the Beaufort Gyre circulation is too weak (Willmes & Heinemann, 2016), there are too few mesoscale eddies (Zhao et al., 2014), or that the ice-ocean drag parameterization that does not take into account keels and sails in deformed multi-year ice is too simple (Tsamados et al., 2014; Castellani et al., 2018).

P14 Figure 6: over what period? Season? Specify in caption

The period of all statistics presented in the manuscript is the entire RGPS period (winters 1996 to 2008). We added this to the figure caption to be more clear:

Figure 6. (a,b,c) Mean orientation of LKFs for RGPS and two model simulations for the winters between 1996 and 2008. ...

P15L7: good review

Thank you.

P15L12: So not clear what method you use to measure LKF lengths

The length of the LKF is given by summing the distances between the individual pixels of the LKF. We added this information to the manuscript:

We determine the PDF of LKF lengths from RGPS data and both model simulations (Fig. 7a). The LKF length is measured as the cumulative sum of the distance between pixels along the LKF.

P16L29: Cite also study by Hibler and Hutchings, 2004, + several studies by Wilchinsky + Feltham + Tsamados + Heorton on anisotropic rheology with prescribed diamond shaped floes. Tsamados et al, 2013 describes sensitivity to this intersection angle See also papers by Cunningham et al, 1994, Schulson et al, 2006, but also Gray, Coon, Pritchard, Maslowski, Ukita, Moritz...

We acknowledge that there are plenty of studies dealing with intersection angles of deformation lines and thank the reviewer to highlight a few. Given that the referred section deals with the disagreement of modeled and observed intersection angles, there are three different categories of papers that we would like to cite: (i) studies of observed intersection angles, (ii) studies that link the intersection angle to the material properties of the ice (namely the rheology), (iii) studies that modeled deformation lines and compared intersection angles. We added for (i) Cunningham et al. (1994) and Schulson et al. (2006), for (ii) Utika and Moritz (1995) (we already cited the suggested Pritchard, 1988), and for (iii) Hutchings et al. (2005).

The papers on the anisotropic rheology deal with the parameterisation of given intersection angles on subgrid scale. In the paper, however, we study the intersection of grid-scale LKFs simulated by the model. We do not see how both can be related despite the high quality of named studies. Therefore, we refrain from citing them in this part of the manuscript.

The paragraph now reads as follows:

The PDF of intersection angles for RGPS data peaks around 40°-50° (Fig. 9). This peak agrees with typical intersection angles of 30°-50° inferred from satellite imagery (Walter and Overland, 1993; Cunningham et al., 1994; Schulson, 2004; Wang, 2007) and laboratory measurements (Schulson et al.,

2006). We find the lowest probabilities for angles smaller than  $20^\circ$ . Angles larger than  $50^\circ$  occur more often than angles smaller than  $40^\circ$ . The distributions of intersection angles in both model simulations are very different from the RGPS data and peak at  $90^\circ$ , which is in agreement with idealized experiments using the VP rheology (Hutchings et al., 2005). Intersection angles smaller than  $60^\circ$  are less frequent in the model simulations than in the RGPS data. The differences between both simulations are small. According to theoretical considerations, the intersection angle is determined by the slope of the yield curve (Pritchard, 1988; Ukita and Moritz, 1995; Wang, 2007). As both simulations use the same elliptical yield curve with a normal flow-rule (Hibler, 1979) similar intersection angles of LKFs are expected. We attribute the small differences in Fig. 9 to sea ice fields with a different amount of LKFs. Ringeisen et al. (2019) derived for idealized compression experiments that it is impossible to obtain intersection angles smaller than  $60^\circ$  with an elliptical yield curve. This explains the deficit of small intersection angles in our simulations.

**P17 figure 9: So quite important structural difference of the model with reality here.**

Therefore we summarize: *“Although the model reproduces most LKF statistics, it completely fails to simulate the observed distribution of LKF intersection angles.”* in the Discussions.

**P18L5: angles**

Changed accordingly.

**P18L17: define lifetime calculation (algo).**

We added information to make it clearer:

We determine the lifetime of an LKF by counting how many times we track a feature. The lifetime estimates are binned into 3-day intervals, that is, the temporal resolution of the deformation data. If an LKF can not be tracked, we assign it to the lowest lifetime class (0-3 days). Tracked LKFs are assigned to a lifetime class according to the number of tracks (one time tracked is assigned to 3-6 days, two time tracked to 6-9 days, etc.).

**How model resolution is this?**

As discussed already in the answer to the major comment, the temporal resolution of 120s is much smaller than the smallest lifetime regarded (0-3 days). Thus we do not expect that the presented PDF of lifetimes is impacted by the choice of temporal resolution.

**Do you calculate persistence in a lagrangian or eulerian way?**

As we track feature in time using the drift information, our persistence can be regarded as Lagrangian quantity.

**P18L32: Why didn't you estimate similar biases for the other LKFs characteristics discussed earlier?**

The bias the reviewer refers to is an uncertainty in the tracked features caused by the temporal varying spatial coverage of the RGPS data-set. This primarily impacts all LKF characteristics that are based on the result of the tracking algorithm, that are, LKF persistence and growth rates. For both quantities, we already discuss the effects of this uncertainty.

**P22L19: or indirectly in the anisotropic rheologies of Tsamados et al, 2013 via the additional dynamics on the order parameter controlling the degree of anisotropy**

We added:

Note that the local degree of anisotropy of the elastic-anisotropic plastic rheology (Tsamados et al. 2013) also represents a memory of past deformation.

P22L32: see also Heorton et al, 2019

Please see comment above for new literature in the section of intersection angles.

## References:

Cunningham, G. F., Kwok, R., and Banfield, J.: Ice lead orientation characteristics in the winter Beaufort Sea, in: Proceedings of IGARSS '94 - 1994 IEEE International Geoscience and Remote Sensing Symposium, vol. 3, pp. 1747–1749 vol.3, <https://doi.org/10.1109/IGARSS.1994.399553>, 1994.

Haas, C.: Dynamics Versus Thermodynamics: The Sea Ice Thickness Distribution, chap. 4, pp. 113–151, John Wiley Sons, Ltd, <https://doi.org/10.1002/9781444317145.ch4>, <https://onlinelibrary.wiley.com/doi/abs/10.1002/9781444317145.ch4>, 2010.

Heorton H. D. B. S., Feltham D. L. and Tsamados M., Stress and deformation characteristics of sea ice in a high-resolution, anisotropic sea ice model; *Philosophical Transactions of the Royal Society A: Mathematical, Physical and Engineering Sciences*; <http://doi.org/10.1098/rsta.2017.0349>; 2018

Horvat, C., E. Tziperman, and J.-M. Campin (2016), Interaction of sea ice floe size, ocean eddies, and sea ice melting, *Geophys. Res. Lett.*, 43, 8083–8090, doi:10.1002/2016GL069742.

Horvat, C., Roach, L., Tilling, R., Bitz, C., Fox-Kemper, B., Guider, C., Hill, K., Ridout, A., and Sheperd, A.: Estimating The Sea Ice Floe Size Distribution Using Satellite Altimetry: Theory, Climatology, and Model Comparison, *The Cryosphere Discuss.*, <https://doi.org/10.5194/tc-2019-134>, in review, 2019.

Hutchings, J. K., Heil, P., and Hibler, W. D.: Modeling Linear Kinematic Features in Sea Ice, *Monthly Weather Review*, 133, 3481–3497, <https://doi.org/10.1175/MWR3045.1>, <https://doi.org/10.1175/MWR3045.1>, 2005.

Hutter, N.: Viscous-plastic sea-ice models at very high resolution, Master's thesis, University of Bremen, Alfred Wegener Institute, Helmholtz Centre for Polar and Marine research, <https://doi.org/10013/epic.46129>, <http://dx.doi.org/10013/epic.46129>, 2015

Koldunov, N. V., Danilov, S., Sidorenko, D., Hutter, N., Losch, M., Goessling, H., et al. (2019). Fast EVP solutions in a high-resolution sea ice model. *Journal of Advances in Modeling Earth Systems*, 11, 1269–1284. <https://doi.org/10.1029/2018MS001485>

Kwok, R. and Cunningham, G. F.: RADARSAT GEOPHYSICAL PROCESSOR SYSTEM: DATA USER'S HANDBOOK (Version 2.0), 2014.

Levy, G., Coon, M., Nguyen, G., and Sulsky, D.: Metrics for evaluating linear features, *Geophysical Research Letters*, 35, <https://doi.org/10.1029/2008GL035086>, <https://agupubs.onlinelibrary.wiley.com/doi/abs/10.1029/2008GL035086>, 2008.

Lüpkes, C. and Gryanik, V. (2015): Parameterization of drag coefficients over polar sea ice for climate models, *Mercator Ocean Quarterly Newsletter - Special Issue*, 51, pp. 29-34.

Manucharyan, G. E., & Thompson, A. F. (2017). Submesoscale sea ice-ocean interactions in marginal ice zones. *Journal of Geophysical Research: Oceans*, 122, 9455–9475.  
<https://doi.org/10.1002/2017JC012895>

Menemenlis, D., I. Fukumori, and T. Lee (2005), Using Green's functions to calibrate an ocean general circulation model, *Mon. Weather Rev.*, 133(5), 1224–1240, doi:[10.1175/MWR2912.1](https://doi.org/10.1175/MWR2912.1).

Mohammadi-Aragh, M., Goessling, H. F., Losch, M., Hutter, N., and Jung, T.: Predictability of Arctic sea ice on weather time scales, *Scientific reports*, 8, 2018.

Schulson, E., Fortt, A., Iliescu, D., and Renshaw, C.: On the role of frictional sliding in the compressive fracture of ice and granite: Terminal vs. post-terminal failure, *Acta Materialia*, 54, 3923 – 3932,  
<https://doi.org/https://doi.org/10.1016/j.actamat.2006.04.024>,  
<http://www.sciencedirect.com/science/article/pii/S1359645406003120>, 2006.

Sumata, H., F. Kauker, M. Karcher, and R. Gerdes, 2019: [Simultaneous Parameter Optimization of an Arctic Sea Ice–Ocean Model by a Genetic Algorithm](https://doi.org/10.1175/MWR-D-18-0360.1). *Mon. Wea. Rev.*, 147, 1899–1926,  
<https://doi.org/10.1175/MWR-D-18-0360.1>

Ukita, J., and R. Moritz (1994), Yield curves and flow rules of pack ice, *Journal of Geophysical Research-Oceans*, 100(C3), 4545–4557.

Tsamados, M., Feltham, D. L., and Wilchinsky, A. V.: Impact of a new anisotropic rheology on simulations of Arctic sea ice, *Journal of Geophysical Research: Oceans*, 118, 91–107,  
<https://doi.org/10.1029/2012JC007990>, <https://agupubs.onlinelibrary.wiley.com/doi/abs/10.1029/2012JC007990>, 2013.

Ukita, J. and Moritz, R. E.: Yield curves and flow rules of pack ice, *Journal of Geophysical Research: Oceans*, 100, 4545–4557, <https://doi.org/10.1029/94JC02202>,  
<https://agupubs.onlinelibrary.wiley.com/doi/abs/10.1029/94JC02202>, 1995

Wadhams, P.: Sea ice thickness distribution in the Greenland Sea and Eurasian Basin, May 1987, *Journal of Geophysical Research: Oceans*, 97, 5331–5348, <https://doi.org/10.1029/91JC03137>,  
<https://agupubs.onlinelibrary.wiley.com/doi/abs/10.1029/91JC03137>, 1992.

Zhao, M., Timmermans, M.-L., Cole, S., Krishfield, R., Proshutinsky, A., and Toole, J.: Characterizing the eddy field in the Arctic Ocean halo- cline, *Journal of Geophysical Research: Oceans*, 119, 8800–8817,  
<https://doi.org/10.1002/2014JC010488>, <https://agupubs.onlinelibrary.wiley.com/doi/abs/10.1002/2014JC010488>, 2014.